

Knowledge from Large-Scale Protein Contact Prediction Models Can Be Transferred to the Data-Scarce RNA Contact Prediction Task

Yiren Jian ^{† 1} Chongyang Gao ² Chen Zeng ³ Yunjie Zhao ⁴ Soroush Vosoughi ^{† 1}

Abstract

RNA, whose functionality is largely determined by its structure, plays an important role in many biological activities. The prediction of pairwise structural proximity between each nucleotide of an RNA sequence can characterize the structural information of the RNA. Historically, this problem has been tackled by machine learning models using expert-engineered features and trained on scarce labeled datasets. Here, we find that the knowledge learned by a protein-coevolution Transformer-based language model can be transferred to the RNA contact prediction task. As protein datasets are orders of magnitude larger than those for RNA contact prediction, our findings and the subsequent framework greatly reduce the data scarcity bottleneck. Experiments confirm that RNA contact prediction through transfer learning using a publicly available protein language-model is greatly improved. *Our findings indicate that the learned structural patterns of proteins can be transferred to RNAs, opening up potential new avenues for research.* The code and data (for inference and training) are available for review at <https://anonymous.4open.science/r/ICML2024-submission-792>, which we will make public available after review.

1. Introduction

Proteins and RNAs are critical to many biological processes such as coding, regulation, and expression (Sharma et al., 2016; Goodarzi et al., 2015; Esteller, 2011; Shi et al., 2016; Fire et al., 1998). Understanding their structures is key to de-

ciphering their functionalities. While experimental methods like X-ray diffraction (Stubbs et al., 1977), nuclear magnetic resonance (NMR) (Cavalli et al., 2007), and Cryogenic electron microscopy (Cryo-EM) (Glaeser, 2016) can determine 3D structures, it remains challenging for structurally flexible molecules, e.g., RNAs (Ma et al., 2022). Consequently, the Protein Data Bank has limited RNA structures cataloged (Berman et al., 2000).

In response, many computational tools for 3D structure prediction of biological molecules have been developed in the last decade (Leaver-Fay et al., 2011; Yang et al., 2015; 2020; Källberg et al., 2012). Recently, deep neural networks such as AlphaFold (Jumper et al., 2021), ProteinMPNN (Dau-
paras et al., 2022), RoseTTAFold (Baek et al., 2021), and Metagenomics (Lin et al., 2022) have revolutionized 3D protein structure prediction, partly due to their large size and training datasets. However, this progress has not been paralleled for RNAs, mainly due to the scarcity of RNA datasets. Current RNA datasets are significantly smaller than protein datasets, with well-curated datasets containing less than 100 RNAs (Zerihun et al., 2021) and models trained on fewer than 300 RNA structures (Sun et al., 2021; Zhang et al., 2021b). These small datasets are insufficient for training large deep neural networks, leading to RNA 3D prediction tools based on simulations (SimRNA, Rosetta FARFAR, iFoldRNA, NAST) (Boniecki et al., 2016; Das et al., 2010; Krokhutin et al., 2015; Jonikas et al., 2009; Shi et al., 2015) or fragment assembly (ModeRNA, Vfold, RNAComposer, 3dRNA) (Rother et al., 2011; Xu et al., 2014; Popenda et al., 2012; Zhao et al., 2012; Wang et al., 2019). In the absence of powerful 3D structure prediction models, certain structural properties of RNAs can be determined through RNA Contact Prediction (Jian et al., 2019). The contact predictions can be used as an intermediary step to facilitate the prediction of 3D structures or directly for downstream tasks that rely on RNA structural information. For an RNA sequence of length L , this task aims at predicting a $L \times L$ symmetric binary matrix (called contact map) where a value of 1 at position (i, j) indicates that the i^{th} and j^{th} nucleotides are in contact¹ with each other to each other

¹Department of Computer Science, Dartmouth College

²Department of Computer Science, Northwestern University

³Department of Physics, The George Washington University

⁴Institute of Biophysics, Central China Normal University. Correspondence to: Yiren Jian <yiren.jian.gr@dartmouth.edu>, Soroush Vosoughi <soroush.vosoughi@dartmouth.edu>.

¹Contact is defined as distances smaller than a specific threshold. Following prior works, this is set by a hard distance threshold of 10 Å.

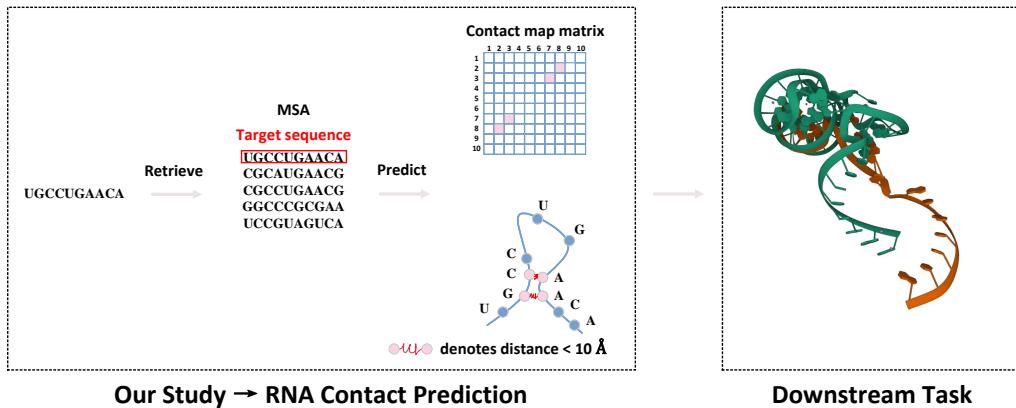


Figure 1. Our study is focused on RNA contact prediction, i.e., predicting the contact map matrix for an RNA sequence. The contact map indicates the proximity between each nucleotide, with those closer than a threshold (10 Å) being deemed in contact. Correct predictions of the contact map can benefit downstream tasks, e.g., by acting as constraints for filtering 3D RNA structure predictions.

in 3D space. The predicted contact maps capture structural constraints, which can be used for downstream tasks, such as refining RNA 3D prediction tools (Wang et al., 2019) (see Figure 1 for an overview of the task). Note that for a target RNA sequence, the input for an RNA contact prediction model is an RNA multiple sequence alignment (MSA), which corresponds to the target RNA sequence stacked with known homologous sequences.

The first RNA Contact Prediction attempt was Direct Coupling Analysis (DCA), with variants like mfDCA (Morcos et al., 2011), mpDCA (Weigt et al., 2009), plmDCA (Ekeberg et al., 2013), bmDCA (Muntoni et al., 2021), and PSI-COV (Jones et al., 2012). These self-supervised methods infer contact maps using maximum likelihood estimation without labeled datasets. Recently, supervised methods have been explored to improve RNA contact prediction. Due to the small number of available RNA-contact map pairs, these methods rely on feature engineering, such as in RNA-contact (Sun et al., 2021), which uses covariance matrices from Infernal (Nawrocki & Eddy, 2013), PETfold-predicted secondary structures (Seemann et al., 2011), and RNAsol solvent accessible surface areas (Sun et al., 2019) to train a deep ResNet model (He et al., 2016). Zerihun et al. (2021) found that simple DCA outputs re-weighted by a convolutional layer (CoCoNet) achieve comparable RNA contact prediction precision (Zerihun et al., 2021).

Supervised RNA contact prediction methods leverage additional knowledge from RNA analytic tools for more informative features. These small models are necessitated by limited training examples. In contrast, abundant protein data allowed for training a large Transformer-based deep neural network, Co-evolution Transformer (CoT), for protein contact prediction (Zhang et al., 2021a). CoT was trained on 90K curated protein structures, compared to ≤ 100 RNA

structures.

Since we lack the data to train such a model for RNA contact prediction from scratch, we investigate the possibility of re-using and tuning the learned parameters of a pre-trained protein language-model (such as CoT) to create an RNA contact prediction model, a process referred to as transfer learning. Inspired by recent breakthroughs in unified vision-language models (Bao et al., 2022; Wang et al., 2022; Li et al., 2021) and transfer learning across text and visual domains (Lu et al., 2021; Jian et al., 2022), which have demonstrated the effectiveness of transferring knowledge between related modalities, such as leveraging the structural abilities learned from code and music to enhance language models (Papadimitriou & Jurafsky, 2020), we propose that bio-molecule contact patterns learned by the CoT protein Transformer network could be transferred to improve RNA contact prediction performance.

Similar to RNA contact prediction models, CoT takes protein MSAs as input. The input to CoT is represented using English characters, with each amino acid represented by a unique English character. CoT then utilizes the attention mechanism of Transformers (Vaswani et al., 2017) to learn the contacts, analogous to how Transformer-based language models, such as GPT-3 (Brown et al., 2020), learn dependencies between words in a given text. Though at the surface level, RNA and protein sequence data are comprised of different building blocks (nucleotides for RNAs and amino acids for proteins), we speculate that they share deeper similarities concerning their contact patterns, analogous to two languages with different lexicons but a similar syntax. Hence, it may be possible to transfer knowledge about contact patterns from one to another, analogous to cross-lingual transfer in Transformer-based language models (Gogoulou et al., 2022).

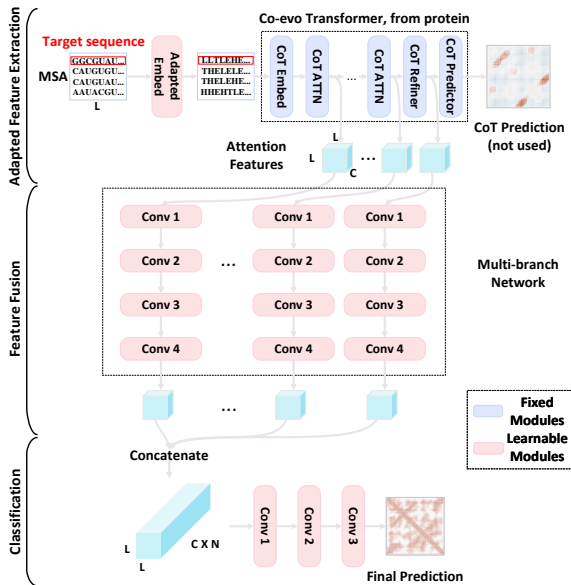


Figure 2. Overview of our three-stage method (from top to bottom). **Adapted Feature Extraction:** First, a projection layer is used to translate the RNA MSA sequences into protein language (e.g., from nucleotide “AUCG” to amino acids “HETL”). Then, we leverage a fixed large-scale pre-trained protein contact prediction transformer model (called Co-evolution Transformer model (CoT)) to extract attentive (i.e., contribution) features at different layers. **Feature Fusion:** Features from different layers are processed by separate convolution blocks before being concatenated. **Classification:** The aggregated features are sent into a standard Convolutional Network (ConvNet) classifier with three layers of convolution.

We investigate our hypothesis by adapting the pre-trained CoT to our RNA dataset and using the adapted representations to train a convolutional network (ConvNet) for RNA contact prediction (see Figure 2 for an overview of our method). Our explorations show that this simple method, which does not rely on any additional pre-processing or feature engineering and can detect true contacts missed by prior works. In addition to improving RNA contact prediction by using knowledge from a pre-trained protein language-model, **more importantly, our study serves as a strong proof of concept for the possibility of transfer learning between the proteins and RNAs.**

2. Background and Related Works

Unsupervised Contact Prediction Based on the Co-Evolution Hypothesis The *co-evolution hypothesis* is the basis of many contact prediction methods (for both proteins and RNA). The hypothesis suggests that spatially proximate pairs of amino acids or nucleotides tend to co-evolve to maintain their structure and function (Weigt et al., 2009).

In practice, this is used for RNA (and protein) contact prediction as follows: to predict the contacts of a target RNA sequence, first, a sequence database is used to find similar sequences. These sequences are likely homologs of the target, with differences due to mutations during evolution. These sequences are then aligned, creating what is called a multiple sequence alignment (a.k.a MSA). Based on the co-evolution hypothesis, the contact prediction for the target sequence can then be reformulated as detecting the co-evolution nucleotide pairs in the MSA. For example, Morcos et al. (2011) calculate the covariance between each pair of nucleotides, thus creating a covariance matrix as an approximation of the co-evolution. The direct coupling score (DCA score) between each pair can then be computed through different approximation methods. While Morcos et al. (2011) use mean-field approximation (mfDCA), other DCA variants (e.g., (Ekeberg et al., 2013)) use different tricks for the approximation.

DCA methods are all purely unsupervised, based on the counting frequency of the residues in MSA, and can be applied to proteins and RNA sequences. Recently, it has been shown that transformer-based protein language-models can also be unsupervised protein contact learners (Rao et al., 2021a;b), though these methods are not necessarily based on the co-evolution hypothesis.

Supervised Contact Prediction Given $\sim 180K$ known protein structures in PDB, Zhang et al. (2021a) train a 20M-parameters attention-based Transformer model for end-to-end prediction of protein contacts based on MSA. The attention mechanism of the model, called the Co-evolution Transformer (CoT), is specifically designed to model co-evolution by considering the outer product of representations of two positions. Such a model is only successful given a large labeled dataset of known MSA to contact mappings.

Training such a large model for RNA is unfortunately not practical as there are currently no such large datasets available. The largest of such data is at least 2-3 orders of magnitude smaller than what is available for proteins. To overcome this bottleneck, most resort to feature engineering to train smaller models. For instance, recent works (Zhang et al., 2021b; Sun et al., 2021) combine DCA outputs (or similarly, covariance matrices) with other features (such as predicted secondary structures, solvent surface areas, etc.) extracted from different RNA analysis tools to train relatively small convolution networks, using only hundreds of labeled data point. Then, Zerihun et al. (2021) propose CoCoNet, showing that the output of DCA by itself is sufficient for training such models and that oftentimes expensive additional feature extraction is not needed. Finally, a recent work (Taubert et al., 2023) investigates self-supervised training with regression for RNA contact prediction.

Transfer Learning We show in this paper that the learned knowledge of a pre-trained protein contact prediction model can be effectively used for RNA contact prediction, not only removing the need for additional feature engineering and extraction but also vastly outperforming CoCoNet. Our proposed method is built upon the concept of “Transfer Learning” (Donahue et al., 2014), which assumes that knowledge learned from one task is beneficial to other related tasks. Transfer learning has enabled the adaption of large pre-trained deep neural networks to new tasks with a limited number of labeled examples. This is typically done by training newly initialized layers at the end of the pre-trained network (which tends to be task-specific) using the small dataset while keeping the other layers frozen (which preserves the learned knowledge from the previous task). Only the relatively small set of parameters in the final layers will be updated, which will adapt the network to the new task.

Transfer Learning has been shown to be effective for class-level transfer in a single domain (Wah et al., 2011) and for different domains (e.g., an image classification model adapted for semantic segmentation (Long et al., 2015)). There is also research that shows that seemingly unrelated tasks can also help each other (Meyerson & Miikkulainen, 2021). Even models for different modalities can be transferred. For instance, Mokady et al. (2021) and Lu et al. (2021) show that semantic knowledge can be transferred between language and visual models.

A key challenge of RNA contact prediction is the small dataset size, which prohibits us from learning a deep model from scratch. We hypothesize (and later verify) that knowledge could be effectively transferred from a pre-trained protein contact Transformer to RNA contact prediction, enabling us to train high-performing RNA contact prediction models without the need for additional labeled or feature engineering, both of which can be prohibitively expensive. Analogies can be drawn between our approach and research done on the cross-lingual transfer of language models (Gogoulou et al., 2022) that adapt a pre-trained model to a new language by learning its syntax while retaining the semantic knowledge in the pre-trained model; here we are adapting a biological model pre-trained on the “language of proteins” to the “language of RNAs”.

3. Methods and Setups

3.1. Protein-to-RNA Transferred Contact Prediction Model

In this section, we provide details of our model’s architecture, input, and output. An overview of our approach is visualized in Figure 2.

3.1.1. MSA AS INPUT

Our RNA contact prediction model relies on the CoT model, which takes protein MSA as the input. Thus, we need to adapt or map the RNA language, which is comprised of nucleotides, to the protein language, which is comprised of amino acids. Specifically, suppose our target RNA MSA has M aligned sequences, each with the length of L nucleotides. Then, the RNA MSA can be represented as a $M \times L$ matrix, with each element being “A”, “U”, “C”, “G”, “-”, where “-” denotes a gap in the alignment. As the CoT embedding layer recognizes only symbols corresponding to amino acids and not nucleotides, we assign each type of nucleotide in the RNA MSA to an amino acid symbol. For example, we could take a random translation from “A”, “U”, “C”, “G” to “H”, “E”, “T”, “L”, to get the following translation:

$$\begin{aligned} \text{“A”} & (\text{Adenine}) \rightarrow \text{“H”} (\text{Histidine}) \\ \text{“U”} & (\text{Uracil}) \rightarrow \text{“E”} (\text{Glutamic Acid}) \\ \text{“C”} & (\text{Cytosine}) \rightarrow \text{“T”} (\text{Threonine}) \\ \text{“G”} & (\text{Guanine}) \rightarrow \text{“L”} (\text{Leucine}) \end{aligned}$$

As we show in our experiments, a random translation between nucleotide and amino acid symbols would be sufficient for adapting the protein contact prediction model, CoT, to RNA contact prediction. However, as discussed in Section 4.2.4, smarter translations, which can be manually devised or learned, could result in a better performance for our adapted RNA contact prediction model.

3.1.2. THE LEARNABLE MODEL

The CoT model has six consecutive attention blocks and one refinement block, each outputting a $L \times L \times C$ attentive feature map, where C is a hyper-parameter corresponding to the number of features being learned by the model. In the original implementation of the protein CoT, C is set to 96, and the output of each attention block (i.e., the feature map for that block) is fed into the next block (see the “Adapted Feature Extraction” row in Figure 2).

For our RNA contact prediction, we further attach four layers of 2D convolution (Conv2d) modules to the intermediate feature map outputs for each of the seven attention blocks described above (see the “Feature Fusion” row in Figure 2). We concatenate the output of the Conv2d modules for each of the seven attention blocks into one $L \times L \times (C \times 7)$ tensor and finally pass it to a classifier module with 3 Conv2d layers for contact prediction (see the “classification” row in Figure 2). The output of our model has shape $L \times L \times 37$, i.e., the distance between pairs of nucleotides is divided into 37 bins. Our model is trained using standard cross-entropy loss with the bins as labels. The summed probability value of the bins for a distance less than 10Å is used as the final contact prediction.

The complete architecture of our model is visualized in Figure 2.

3.2. Dataset

We use a publicly-available well-curated RNA dataset used by [Zerihun et al. \(2021\)](#). We use the provided data split for training, validation, and testing. `RNA_DATASET` is used for training (and validation) and `RNA_TESTSET` is for testing. We removed 3 RNAs (RF02540, RF01998 and RF02012) whose sequences are too long for CoT. In total, we have 56 RNAs for training and validation and 23 RNAs for testing, all from different RNA families. We set the maximum number of homology sequences in MSA to be 200, based on the limits of our GPU memory. This constraint can be alleviated if large GPUs are available.

3.3. Baseline Methods

We compare our method to several representative MSA-based methods: (1) Unsupervised methods: mfDCA and plmDCA, using the implementations from `pydca` ([Zerihun et al., 2020](#)), and PSICOV ([Jones et al., 2012](#)), and PLMC ([Hopf et al., 2017](#)) (2) Supervised method: CoCoNet.

Note that all these baselines are variants of DCA or are based on DCA (the current trend in studying RNA contacts). Our proposed method does not rely on DCA and approaches the problem from a different angle through the transfer learning of learned knowledge from a pre-trained protein contact prediction model.

3.4. Training Details

We use the Adam optimizer ([Kingma & Ba, 2015](#)) and cosine anneal learning rate scheduler with an initial learning rate of $1e^{-3}$. We train on an RTX-A6000 GPU using PyTorch-1.8 and CUDA-11 and search the hyper-parameters for the total training epochs among $\{100, 300, 500\}$ and batch sizes among $\{4, 8, 12, 16\}$. The code is available for review at <https://anonymous.4open.science/r/ICML2024-submission-792>.

We randomly divide the 56 RNAs reserved for training into 47 RNAs for training and 9 RNAs for validation and use the given 23 RNAs in the test dataset for testing. The best-validated model during the training is used for testing. See Appendix A for details of the validation splits.

3.5. Evaluation Metrics

Following the standard protocol of prior works ([Jian et al., 2019](#); [Zhang et al., 2021b](#); [Sun et al., 2021](#); [Singh et al., 2022](#)), we evaluate the precision on each RNA sequence of length L with top- L predictions of each method (PPV_L); i.e., for an RNA with a sequence of length L , we use our

Method	PPV_L	$PPV_{0.5L}$	$PPV_{0.3L}$
mfDCA	34.1	46.7	57.4
plmDCA	30.6	43.2	57.8
PSICOV	32.1	43.8	57.8
PLMC	33.5	45.9	57.4
CoCoNet [§] (3×3)	61.6	67.7	69.1
CoCoNet [§] (5×5)	61.8	65.2	67.8
CoCoNet [§] (7×7)	62.4	66.6	69.2
CoCoNet ^{§¶} $(3 \times 3) \times 2$	67.1	71.6	72.3
CoCoNet ^{§¶} $(5 \times 5) \times 2$	67.5	71.9	75.0
CoCoNet ^{§¶} $(7 \times 7) \times 2$	68.5	73.2	75.2
CoT-RNA [†] (Ours)	73.5	80.6	83.0
CoT-RNA [†] (average)	72.1 ± 1.1	79.2 ± 1.7	81.9 ± 2.2

Table 1. Comparison of different RNA contact prediction methods based on MSA. [§]: Using the publicly released parameters by [Zerihun et al. \(2021\)](#), which are trained using our training and validation sets. [¶]: Using prior knowledge of Watson-Crick pairs is used. [†]: Our models trained using only the training set, selected based on the best validation and evaluated on the testing set. [‡]: We repeat the experiments four times using different random training and validation splits and report the mean and standard deviation of the results on the test dataset.

model to make L predictions (for all different (i, j) pairs). Among these L predictions, if K pairs are true contacts, then $PPV_L = \frac{K}{L}$. We also report results for $PPV_{0.3/0.5L}$.

4. Results

Unless specified otherwise, the results presented in this manuscript employ translation nucleotides to amino acids (AUCG \rightarrow HETL) as detailed in Sec. 3.1.1.

4.1. Main Results

We first compare our method to those only using MSA as input to evaluate the contribution of the pre-trained protein Transformer to RNA contact prediction. Unsupervised algorithms like mfDCA, plmDCA, PSICOV, and PLMC are based on covariance analysis. CoCoNet uses DCA output as input and ground truth contact maps to train a supervised ConvNet classifier. We compare six CoCoNet configurations from [Zerihun et al. \(2021\)](#).

Table 1 shows supervised models significantly outperform unsupervised baselines. Our transfer learning-based model outperforms the best CoCoNet configuration by an absolute of 5.0, 7.4, and 7.8 for PPV_L , $PPV_{0.5L}$, and $PPV_{0.3L}$, respectively (see Appendix B for contact visualization).

CoCoNet is designed to be shallow, with a few parameters to learn, given the very limited number of available RNA contact prediction training data and features (from DCA). In contrast, by transfer learning of CoT, a large pre-trained protein contact prediction model, our model is much larger and deeper and can learn more diverse features through

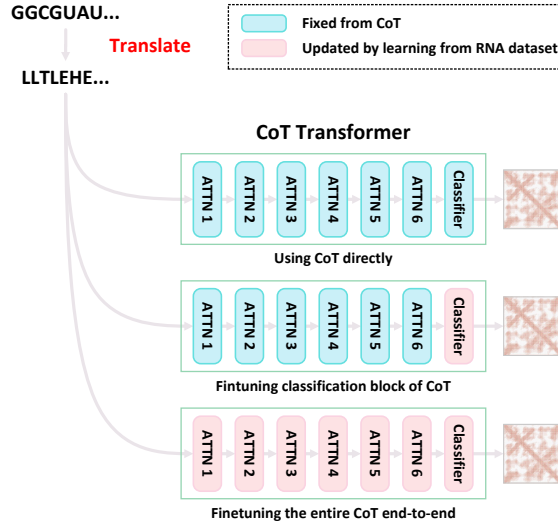


Figure 3. Common baselines for transferring protein CoT to RNA contact prediction.

the multi-layer attentions of CoT contain. To investigate whether the improvement of our model over CoCoNet is mainly based on its capacity or the learned knowledge of the pre-trained protein language-model, we also implement a Deep-CoCoNet, which takes the same inputs as CoCoNet but replaces the CoCoNet’s original shallow ConvNet with a deep model similar to ours (with the same number of layers and each layer with the same number of channels, except for the first input layer). We find that Deep-CoCoNet performs much worse than the original shallow CoCoNet, possibly due to the hardness of fitting a large model that uses features with limited expressiveness (this may also explain why [Zerihun et al. \(2021\)](#) use a shallow convolution network over deeper ones in their implementation).

While CoCoNet takes DCA as input which is a tensor of $1 \times L \times L$ (L being the RNA sequence length), our method, leveraging multi-layer CoT, has diverse attentive features of shape $(7 \times 96) \times L \times L$ (There are 7 layers in CoT and each layer outputs 96 channels/features). These diverse features allow us to learn deeper and larger models that can better generalize. In Section 4.2.3, we further investigate this, showing that our model indeed benefits from increasing the number of parameters in the transfer modules.

Additionally, we compare our methods with hybrid approaches and RNA secondary predictions in Appendix C and Appendix D, respectively.

4.2. Ablation Studies

Here, we examine the design choices of our model for transfer learning by exploring different configurations.

4.2.1. COMMON TRANSFER LEARNING STRATEGIES

We investigate three common transfer learning strategies (see Figure 3 for an overview) and show that they are not well-suited for this task:

Using CoT directly (CoT directly). By adapting the embedding to map RNA nucleotides to protein amino acids, the pre-trained CoT can directly output a prediction of a distance map for RNA contact prediction without any model modifications.

Fine-tuning the classification block of CoT (CoT cls fine-tuned). A typical approach in transfer learning is to fine-tune the last few layers of a model. CoT has six attention blocks followed by a final ResNet block for prediction. We attach a new classification block while keeping others fixed.

Fine-tuning the entire CoT end-to-end (CoT end-to-end). Another common protocol for transfer learning is to fine-tune the entire pre-trained model end-to-end. We update all parameters in the pre-trained protein CoT by the RNA training set.

Table 2 shows the performance of these methods on our dataset. With a PPV_L of 30.4, the direct use of CoT (CoT directly) without any learning is shown to be inefficient. This suggests that learned protein knowledge by itself cannot be successfully transferred to RNA tasks without some fine-tuning. The results for transfer learning through fine-tuning the classification block of CoT (CoT cls fine-tuned) are considerably better, being competitive with the mfDCA baseline. These results suggest that tuning the attention features in the last layer of CoT enables the transfer of knowledge to the RNA tasks to some extent. However, as this configuration ignores the attention features from the other layers, it performs significantly worse than our method, suggesting that these features also play an important role in contact prediction and need to be tuned for RNA contact prediction. Finally, the end-to-end model, which updates all the parameters in CoT (CoT end-to-end), performs similarly to the last variant. Though this model does not ignore any part of the CoT, it requires the tuning of $\sim 20M$ parameters. With only 56 RNA training points, the model is likely to over-fit.

From these experiments, we can conclude that the effective transfer of protein CoT to the RNA contact prediction task requires (1) adapting some of the parameters of CoT to the new task, (2) leveraging the multi-layer attention features from CoT, and (3) making the number of learnable parameters “small” and proportional to the size of the training set for the new task. These findings lead to our final model design described in Section 3.1.2 that leverages multi-layer attention features from CoT and learns an appropriate number of parameters for our small training set.

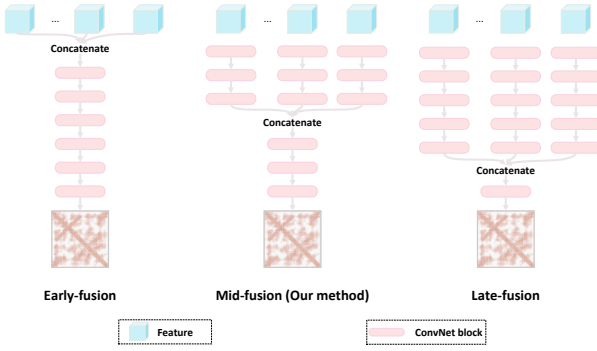
Method	PPV _L	PPV _{0.5L}	PPV _{0.3L}
mfDCA (baseline)	34.1	46.7	57.4
CoT directly	30.4	33.1	34.0
CoT cls fine-tuned	38.3	41.6	41.2
CoT end-to-end	36.2	43.2	46.6
Ours	73.5	80.6	83.0

Table 2. Common transfer learning strategies applied to CoT.

Method	PPV _L	PPV _{0.5L}	PPV _{0.3L}
early-fusion	71.8	79.5	82.4
mid-fusion (Ours)	73.5	80.6	83.0
late-fusion	72.0	77.7	79.4

Table 3. Comparison of different feature fusion designs. We modify the number of channels in each layer so that all three models have a similar number of parameters for fair comparison.

4.2.2. FEATURE FUSION DESIGN CHOICES

Figure 4. Different feature fusion strategies. Our final model (shown in Figure 2) uses the *mid-fusion* design.

We examine various strategies for combining attention features from different CoT layers/blocks. Our model, as shown in Figure 2, employs multi-branch networks (each with 4 ConvNet layers) followed by a shared 3-layer ConvNet classification block. Each branch network separately processes the attention features of CoT at each layer, before being fused and passed into the classification block (termed *mid-fusion* design). Other designs include *early-fusion* and *late-fusion*. Early-fusion concatenates all CoT features from different layers and processes them using a single shared network. Late-fusion has separate branch networks for each CoT layer's features before being merged at the very end, followed by a single classification layer. Figure 4 provides a schematic diagram of these three fusion strategies.

To make the comparison of these three designs fair, we modify the number of channels in each layer so that the three models have a similar number of parameters. As shown in Table 3, while all design choices work well, *mid-fusion* has the best performance. It is possible that features from different layers contain different types of information

Method	PPV _L	PPV _{0.5L}	PPV _{0.3L}
Ours (small)	71.1	76.0	79.0
Ours	73.5	80.6	83.0
Ours (large)	78.3	82.3	86.1

Table 4. Comparison of our model with different sizes. While maintaining the network structures, we vary the number of channels in each layer so that we end up with models with different numbers of parameters.

that may need to be processed by different “expert” models (i.e., ConvNet branches in our model), making an *early-fusion* model inefficient. In both *mid-fusion* and *late-fusion*, each branch network will process the attention features of each layer separately, with *late-fusion* having a relatively smaller classification head. The overall better performance of *mid-fusion* suggests that a good design choice is to have a balanced distribution of parameters into the branch networks and the classification head.

These experiments provide insights into the design of hybrid RNA contact prediction methods (Zhang et al., 2021b; Sun et al., 2021; Singh et al., 2022), which all adopt the *early-fusion* design. We further discuss this in Section 5.

4.2.3. DIFFERENT MODEL SIZES

As discussed in Section 4.1, the deep-CoCoNet variant of CoCoNet under-performs compared to the shallower original CoCoNet, likely due to the limited expressiveness of input DCA features which are single channel with a shape of $[1 \times L \times L]$. In contrast, here we demonstrate that our transferred CoT model allows for learning deeper networks, with its performance improving as we increase the parameters in the transfer modules.

We create larger and smaller versions of our model by increasing and decreasing the number of channels in each layer, respectively. As shown in Table 4, the larger models outperform smaller ones, possibly due to the expressiveness of the CoT features from the 7 different attention blocks.

4.2.4. PROTEIN TO RNA TRANSLATION VARIATIONS

We have used a random translation from RNA nucleotides to protein amino acids (e.g., “AUCG” to “HETL”) in our experiments. Here, we study the effects of different translations on our model’s performance.

The 20 amino acids can be categorized into four groups: (1) electrically charged, (2) polar uncharged, (3) hydrophobic, and (4) special cases. Randomly selecting one from each group generally works well (e.g., “AUCG” \rightarrow “RDSY” and “AUCG” \rightarrow “KDNY” in Table 5), indicating our framework’s robustness to translation choices.

We also test possibly one of the worst translations, “AUCG”

Method	PPV_L	$PPV_{0.5L}$	$PPV_{0.3L}$
AUCG → ACDE	68.6	76.9	82.5
AUCG → HETL	<u>73.5</u>	80.6	83.0
AUCG → RDSY	76.1	81.4	83.4
AUCG → KDNY	77.3	84.5	88.6

Table 5. Results of different translations/translations from nucleotides to amino acids of our transferred CoT. Bold corresponds to the best-performing translation; underline corresponds to the main translation used in the experiments.

→ ACDE”, as it may generate unlikely amino acid chains (e.g., a string of negatively charged residues, as “D” and “E” are negatively charged) and hence CoT will have had limited exposure to such sequences during its pre-training. Though we see a relative performance drop, the results are still comparable to CoCoNet. Appendix E offers a more comprehensive analysis, demonstrating our method’s robustness to various translations. Although the choice of amino acids may slightly impact performance, permutations of amino acid sets yield similar outcomes.

A learnable 4×20 nucleotide-to-amino acid embedding could yield better results but faces implementation challenges, such as requiring powerful GPUs and adapting the original CoT model’s separate binary executable embedding layer to the PyTorch framework.

5. Discussion and Conclusion

We demonstrate the effectiveness of transferring CoT, a pre-trained protein Transformer model for contact prediction, to the RNA contact prediction task using a small curated RNA dataset. Unlike hybrid methods, our approach does not use additional features extracted by RNA analysis tools (e.g., RNAcontact). Incorporating CoT features and RNA features (extracted by tools like RNAcontact) could potentially improve our method’s performance.

Note that even though our method uses a Transformer-based architecture that models attention between every element in a sequence, the maximum sequence length is typically limited due to computational constraints to a few hundred elements. Also, we only sample 200 homologous sequences from the multiple sequence alignment (MSA) of an RNA as input. This sampling process may result in the loss of co-evolutionary information, thus limiting the learning capacity of CoT. Furthermore, instead of utilizing a “manual translation” of CoT with a translation of AUCG → HETL, a “soft-learnable translation” from RNA to proteins (a 4×20 matrix) could potentially yield improved results. Nevertheless, as discussed in Sec. 4.2.4, implementing such an approach currently faces several engineering challenges.

Our ablation experiments on model size suggest that using a larger model and modestly increasing the training set size

may improve predictions. Combining these insights could yield a powerful RNA contact prediction model without requiring large-scale RNA data curation.

Our feature fusion experiments show that mid-fusion outperforms early-fusion and late-fusion. Current hybrid RNA, contact prediction tools, adopt an early-fusion design (Zhang et al., 2021b; Sun et al., 2021; Singh et al., 2022), concatenating DCA features and RNA features into a single tensor, followed by learning a Deep ResNet or ConvNet. Intuitively, features from different RNA tools capture distinct knowledge. Therefore, employing dedicated modules for processing features from each tool and using a mid-to-late fusion strategy could improve hybrid method performance.

Our findings shed light on a compelling representation transfer problem in computational structural biology; specifically, we investigate if structural patterns learned from large-scale protein datasets can be transferred to data-scarce RNA problems, particularly for structural contact predictions. Our results indicate that protein-to-RNA transfer learning can improve RNA model performance, suggesting that other pre-trained protein Transformers, such as MSA-Transformer (Rao et al., 2021b) and ESM (Rao et al., 2021a), could potentially be transferred to RNA for other downstream tasks.

6. Limitations

Note that even though our method uses a Transformer-based architecture that models attention between every element in a sequence, the maximum sequence length is typically limited due to computational constraints to a few hundred elements. Also, we only sample 200 homologous sequences from the multiple sequence alignment (MSA) of an RNA as input. This sampling process may result in the loss of co-evolutionary information, thus limiting the learning capacity of CoT. Furthermore, instead of utilizing a “manual translation” of CoT with a translation of AUCG → HETL, a “soft-learnable translation” from RNA to proteins (a 4×20 matrix) could potentially yield improved results. Nevertheless, as discussed in Sec. 4.2.4, implementing such an approach currently faces several engineering challenges.

Impact Statements

The primary contribution of this study lies in demonstrating the transferability of structural patterns derived from pre-trained protein Transformers to RNA tasks. Specifically, we introduce an algorithm for RNA contact prediction. Our proposed method for RNA contact prediction holds significant promise in advancing the field of RNA 3D structural predictions. This advancement, in turn, has far-reaching implications, including its application in drug design and related areas. However, it is crucial to acknowledge the potential limitations of our method. False predictions made

by our algorithm could result in inaccuracies in RNA structure predictions, thereby exerting a detrimental influence on subsequent downstream tasks.

References

Baek, M., DiMaio, F., Anishchenko, I., Dauparas, J., Ovchinnikov, S., Lee, G. R., Wang, J., Cong, Q., Kinch, L. N., Schaeffer, R. D., et al. Accurate prediction of protein structures and interactions using a three-track neural network. *Science*, 373(6557):871–876, 2021.

Bao, H., Wang, W., Dong, L., Liu, Q., Mohammed, O. K., Aggarwal, K., Som, S., Piao, S., and Wei, F. Vlmo: Unified vision-language pre-training with mixture-of-modality-experts. *Advances in Neural Information Processing Systems*, 35:32897–32912, 2022.

Berman, H. M., Westbrook, J., Feng, Z., Gilliland, G., Bhat, T. N., Weissig, H., Shindyalov, I. N., and Bourne, P. E. The protein data bank. *Nucleic acids research*, 28(1):235–242, 2000.

Boniecki, M. J., Lach, G., Dawson, W. K., Tomala, K., Lukasz, P., Soltysinski, T., Rother, K. M., and Bujnicki, J. M. Simrna: a coarse-grained method for rna folding simulations and 3d structure prediction. *Nucleic acids research*, 44(7):e63–e63, 2016.

Brown, T., Mann, B., Ryder, N., Subbiah, M., Kaplan, J. D., Dhariwal, P., Neelakantan, A., Shyam, P., Sastry, G., Askell, A., et al. Language models are few-shot learners. *Advances in neural information processing systems*, 33:1877–1901, 2020.

Cavalli, A., Salvatella, X., Dobson, C. M., and Vendruscolo, M. Protein structure determination from nmr chemical shifts. *Proceedings of the National Academy of Sciences*, 104(23):9615–9620, 2007.

Das, R., Karanicolas, J., and Baker, D. Atomic accuracy in predicting and designing noncanonical rna structure. *Nature methods*, 7(4):291–294, 2010.

Dauparas, J., Anishchenko, I., Bennett, N., Bai, H., Ragotte, R. J., Milles, L. F., Wicky, B. I., Courbet, A., de Haas, R. J., Bethel, N., et al. Robust deep learning-based protein sequence design using proteinmpnn. *Science*, 378(6615):49–56, 2022.

Donahue, J., Jia, Y., Vinyals, O., Hoffman, J., Zhang, N., Tzeng, E., and Darrell, T. Decaf: A deep convolutional activation feature for generic visual recognition. In *International conference on machine learning*, pp. 647–655. PMLR, 2014.

Ekeberg, M., Lökvist, C., Lan, Y., Weigt, M., and Aurell, E. Improved contact prediction in proteins: using pseudolikelihoods to infer potts models. *Physical Review E*, 87(1):012707, 2013.

Esteller, M. Non-coding rnas in human disease. *Nature reviews genetics*, 12(12):861–874, 2011.

Fire, A., Xu, S., Montgomery, M. K., Kostas, S. A., Driver, S. E., and Mello, C. C. Potent and specific genetic interference by double-stranded rna in *caenorhabditis elegans*. *Nature*, 391(6669):806–811, 1998.

Glaeser, R. M. How good can cryo-em become? *Nature methods*, 13(1):28–32, 2016.

Gogoulou, E., Ekgren, A., Isbister, T., and Sahlgren, M. Cross-lingual transfer of monolingual models. In *Proceedings of the Thirteenth Language Resources and Evaluation Conference*, pp. 948–955, Marseille, France, June 2022. European Language Resources Association.

Goodarzi, H., Liu, X., Nguyen, H. C., Zhang, S., Fish, L., and Tavazoie, S. F. Endogenous tRNA-derived fragments suppress breast cancer progression via ybx1 displacement. *Cell*, 161(4):790–802, 2015.

He, K., Zhang, X., Ren, S., and Sun, J. Deep residual learning for image recognition. In *Proceedings of the IEEE conference on computer vision and pattern recognition*, pp. 770–778, 2016.

Hopf, T. A., Ingraham, J. B., Poelwijk, F. J., Schärfe, C. P., Springer, M., Sander, C., and Marks, D. S. Mutation effects predicted from sequence co-variation. *Nature biotechnology*, 35(2):128–135, 2017.

Jian, Y., Wang, X., Qiu, J., Wang, H., Liu, Z., Zhao, Y., and Zeng, C. Direct: Rna contact predictions by integrating structural patterns. *BMC bioinformatics*, 20(1):1–12, 2019.

Jian, Y., Gao, C., and Vosoughi, S. Non-linguistic supervision for contrastive learning of sentence embeddings. In *Advances in Neural Information Processing Systems*, 2022.

Jones, D. T., Buchan, D. W., Cozzetto, D., and Pontil, M. Psicov: precise structural contact prediction using sparse inverse covariance estimation on large multiple sequence alignments. *Bioinformatics*, 28(2):184–190, 2012.

Jonikas, M. A., Radmer, R. J., Laederach, A., Das, R., Pearlman, S., Herschlag, D., and Altman, R. B. Coarse-grained modeling of large rna molecules with knowledge-based potentials and structural filters. *Rna*, 15(2):189–199, 2009.

Jumper, J., Evans, R., Pritzel, A., Green, T., Figurnov, M., Ronneberger, O., Tunyasuvunakool, K., Bates, R., Žídek, A., Potapenko, A., et al. Highly accurate protein structure prediction with alphafold. *Nature*, 596(7873):583–589, 2021.

Källberg, M., Wang, H., Wang, S., Peng, J., Wang, Z., Lu, H., and Xu, J. Template-based protein structure modeling using the raptortx web server. *Nature protocols*, 7(8):1511–1522, 2012.

Kingma, D. P. and Ba, J. Adam: A method for stochastic optimization. In *ICLR (Poster)*, 2015.

Krokhin, A., Houlihan, K., and Dokholyan, N. V. ifoldrna v2: folding rna with constraints. *Bioinformatics*, 31(17):2891–2893, 2015.

Leaver-Fay, A., Tyka, M., Lewis, S. M., Lange, O. F., Thompson, J., Jacak, R., Kaufman, K. W., Renfrew, P. D., Smith, C. A., Sheffler, W., et al. Rosetta3: an object-oriented software suite for the simulation and design of macromolecules. In *Methods in enzymology*, volume 487, pp. 545–574. Elsevier, 2011.

Li, J., Selvaraju, R., Gotmare, A., Joty, S., Xiong, C., and Hoi, S. C. H. Align before fuse: Vision and language representation learning with momentum distillation. *Advances in neural information processing systems*, 34:9694–9705, 2021.

Lin, Z., Akin, H., Rao, R., Hie, B., Zhu, Z., Lu, W., Smetanin, N., Verkuil, R., Kabeli, O., Shmueli, Y., et al. Evolutionary-scale prediction of atomic level protein structure with a language model. *bioRxiv*, 2022.

Long, J., Shelhamer, E., and Darrell, T. Fully convolutional networks for semantic segmentation. In *Proceedings of the IEEE conference on computer vision and pattern recognition*, pp. 3431–3440, 2015.

Lu, K., Grover, A., Abbeel, P., and Mordatch, I. Pretrained transformers as universal computation engines. *arXiv preprint arXiv:2103.05247*, 2021.

Ma, H., Jia, X., Zhang, K., and Su, Z. Cryo-em advances in rna structure determination. *Signal Transduction and Targeted Therapy*, 7(1):1–6, 2022.

Meyerson, E. and Miikkulainen, R. The traveling observer model: Multi-task learning through spatial variable embeddings. In *ICLR*, 2021.

Mokady, R., Hertz, A., and Bermano, A. H. Clipcap: Clip prefix for image captioning. *arXiv preprint arXiv:2111.09734*, 2021.

Morcos, F., Pagnani, A., Lunt, B., Bertolino, A., Marks, D. S., Sander, C., Zecchina, R., Onuchic, J. N., Hwa, T., and Weigt, M. Direct-coupling analysis of residue coevolution captures native contacts across many protein families. *Proceedings of the National Academy of Sciences*, 108(49):E1293–E1301, 2011.

Muntoni, A. P., Pagnani, A., Weigt, M., and Zamponi, F. adabmdca: adaptive boltzmann machine learning for biological sequences. *BMC bioinformatics*, 22(1):1–19, 2021.

Nawrocki, E. P. and Eddy, S. R. Infernal 1.1: 100-fold faster rna homology searches. *Bioinformatics*, 29(22):2933–2935, 2013.

Papadimitriou, I. and Jurafsky, D. Learning music helps you read: Using transfer to study linguistic structure in language models. In *EMNLP*, pp. 6829–6839, 01 2020. doi: 10.18653/v1/2020.emnlp-main.554.

Popenda, M., Szachniuk, M., Antczak, M., Purzycka, K. J., Lukasiak, P., Bartol, N., Blazewicz, J., and Adamiak, R. W. Automated 3d structure composition for large rnas. *Nucleic acids research*, 40(14):e112–e112, 2012.

Radford, A., Kim, J. W., Hallacy, C., Ramesh, A., Goh, G., Agarwal, S., Sastry, G., Askell, A., Mishkin, P., Clark, J., et al. Learning transferable visual models from natural language supervision. In *International conference on machine learning*, pp. 8748–8763. PMLR, 2021.

Rao, R., Meier, J., Sercu, T., Ovchinnikov, S., and Rives, A. Transformer protein language models are unsupervised structure learners. In *International Conference on Learning Representations*, 2021a.

Rao, R. M., Liu, J., Verkuil, R., Meier, J., Canny, J., Abbeel, P., Sercu, T., and Rives, A. Msa transformer. In *International Conference on Machine Learning*, pp. 8844–8856. PMLR, 2021b.

Rother, M., Milanowska, K., Puton, T., Jeleniewicz, J., Rother, K., and Bujnicki, J. M. Moderna server: an online tool for modeling rna 3d structures. *Bioinformatics*, 27(17):2441–2442, 2011.

Sato, K., Akiyama, M., and Sakakibara, Y. Rna secondary structure prediction using deep learning with thermodynamic integration. *Nature communications*, 12(1):941, 2021.

Seemann, S. E., Menzel, P., Backofen, R., and Gorodkin, J. The petfold and petcofold web servers for intra-and intermolecular structures of multiple rna sequences. *Nucleic acids research*, 39(suppl_2):W107–W111, 2011.

Sharma, U., Conine, C. C., Shea, J. M., Boskovic, A., Derr, A. G., Bing, X. Y., Belleannee, C., Kucukural, A., Serra, R. W., Sun, F., et al. Biogenesis and function of tRNA fragments during sperm maturation and fertilization in mammals. *Science*, 351(6271):391–396, 2016.

Shi, M., Lin, X.-D., Tian, J.-H., Chen, L.-J., Chen, X., Li, C.-X., Qin, X.-C., Li, J., Cao, J.-P., Eden, J.-S., et al. Redefining the invertebrate RNA virosphere. *Nature*, 540(7634):539–543, 2016.

Shi, Y.-Z., Jin, L., Wang, F.-H., Zhu, X.-L., and Tan, Z.-J. Predicting 3D structure, flexibility, and stability of RNA hairpins in monovalent and divalent ion solutions. *Biophysical journal*, 109(12):2654–2665, 2015.

Singh, J., Paliwal, K., Litfin, T., Singh, J., and Zhou, Y. Predicting RNA distance-based contact maps by integrated deep learning on physics-inferred secondary structure and evolutionary-derived mutational coupling. *Bioinformatics*, 38(16):3900–3910, 2022.

Stubbs, G., Warren, S., and Holmes, K. Structure of RNA and RNA binding site in tobacco mosaic virus from 4-Å map calculated from X-ray fibre diagrams. *Nature*, 267(5608):216–221, 1977.

Sun, S., Wu, Q., Peng, Z., and Yang, J. Enhanced prediction of RNA solvent accessibility with long short-term memory neural networks and improved sequence profiles. *Bioinformatics*, 35(10):1686–1691, 2019.

Sun, S., Wang, W., Peng, Z., and Yang, J. RNA inter-nucleotide 3D closeness prediction by deep residual neural networks. *Bioinformatics*, 37(8):1093–1098, 2021.

Szikszai, M., Wise, M., Datta, A., Ward, M., and Mathews, D. H. Deep learning models for RNA secondary structure prediction (probably) do not generalize across families. *Bioinformatics*, 38(16):3892–3899, 2022.

Taubert, O., von der Lehr, F., Bazarova, A., Faber, C., Knechtges, P., Weiel, M., Debus, C., Coquelin, D., Basermann, A., Streit, A., et al. RNA contact prediction by data efficient deep learning. *Communications Biology*, 6(1):913, 2023.

Vaswani, A., Shazeer, N., Parmar, N., Uszkoreit, J., Jones, L., Gomez, A. N., Kaiser, Ł., and Polosukhin, I. Attention is all you need. *Advances in neural information processing systems*, 30, 2017.

Wah, C., Branson, S., Welinder, P., Perona, P., and Belongie, S. The Caltech-UCSD Birds-200-2011 dataset. Technical Report CNS-TR-2011-001, California Institute of Technology, 2011.

Wang, J., Wang, J., Huang, Y., and Xiao, Y. 3drna v2.0: An updated web server for RNA 3D structure prediction. *International Journal of Molecular Sciences*, 20(17):4116, 2019.

Wang, J., Yang, Z., Hu, X., Li, L., Lin, K., Gan, Z., Liu, Z., Liu, C., and Wang, L. GIT: A generative image-to-text transformer for vision and language. *Transactions on Machine Learning Research*, 2022. ISSN 2835-8856. URL <https://openreview.net/forum?id=b4tMhpN0JC>.

Weigt, M., White, R. A., Szurmant, H., Hoch, J. A., and Hwa, T. Identification of direct residue contacts in protein–protein interaction by message passing. *Proceedings of the National Academy of Sciences*, 106(1):67–72, 2009.

Xu, X., Zhao, P., and Chen, S.-J. Vfold: a web server for RNA structure and folding thermodynamics prediction. *PloS one*, 9(9):e107504, 2014.

Yang, J., Yan, R., Roy, A., Xu, D., Poisson, J., and Zhang, Y. The i-Tasser suite: protein structure and function prediction. *Nature methods*, 12(1):7–8, 2015.

Yang, J., Anishchenko, I., Park, H., Peng, Z., Ovchinnikov, S., and Baker, D. Improved protein structure prediction using predicted interresidue orientations. *Proceedings of the National Academy of Sciences*, 117(3):1496–1503, 2020.

Zerihun, M. B., Pucci, F., Peter, E. K., and Schug, A. pydca v1.0: a comprehensive software for direct coupling analysis of RNA and protein sequences. *Bioinformatics*, 36(7):2264–2265, 2020.

Zerihun, M. B., Pucci, F., and Schug, A. Coconet—boosting RNA contact prediction by convolutional neural networks. *Nucleic acids research*, 49(22):12661–12672, 2021.

Zhang, H., Ju, F., Zhu, J., He, L., Shao, B., Zheng, N., and Liu, T.-Y. Co-evolution transformer for protein contact prediction. *Advances in Neural Information Processing Systems*, 34:14252–14263, 2021a.

Zhang, T., Singh, J., Litfin, T., Zhan, J., Paliwal, K., and Zhou, Y. Rnacmap: a fully automatic pipeline for predicting contact maps of RNAs by evolutionary coupling analysis. *Bioinformatics*, 37(20):3494–3500, 2021b.

Zhao, Y., Huang, Y., Gong, Z., Wang, Y., Man, J., and Xiao, Y. Automated and fast building of three-dimensional RNA structures. *Scientific reports*, 2(1):1–6, 2012.

A. Validation Splits

As explained in Section 3, we randomly divide the 56 training RNAs (i.e., RNA_DATASET) into 47 RNAs for training and 9 RNAs for validation. We use the provided 23 test RNAs (i.e., RNA_TESTSET) for testing. The best validated model during training is used for testing.

We provide the validation splits in Table A.1. Most experiments are carried out using Validation Set 1, with the exception that we average the results of the four different runs using all validation splits and report the means and standard deviations in Table 1, in the main paper.

Validation Set 1	Validation Set 2	Validation Set 3	Validation Set 4
RF01510	RF01826	RF00442_1	RF00921
RF01689	RF01831_1	RF00458	RF01051
RF01725	RF01852	RF00504	RF01054
RF01734	RF01854	RF00606_1	RF01300
RF01750	RF01982	RF01750	RF01415
RF01763	RF02001_2	RF01763	RF01510
RF01767	RF02266	RF01767	RF01689
RF01786	RF02447	RF01786	RF01725
RF01807	RF02553	RF01807	RF01734

Table A.1. Validation set partitions.

B. Visual Comparisons Between CoCoNet and Ours

In this section, we present six visual examples comparing the contacts predicted by CoCoNet and those predicted by our method. Intuitively, our improved RNA contact predictions, as depicted in Figure B.1, will provide better guidance for downstream tasks.

C. Comparison with Advanced Hybrid Approaches

Current hybrid methods for RNA contact prediction typically combine DCA with other RNA features (extracted by various RNA analysis tools) and train a supervised classifier using convolution networks. For example, RNAcontact (Sun et al., 2021) combine DCA with three other types of RNA features: (1) Covariance (computed by Infernal, which can be viewed as a variant of DCA), (2) Secondary Structures, either given or predicted by PETFold, (3) Solvent Accessible Area provided by RNAsol.

Running hybrid methods such as RNAcontact locally can be challenging for practitioners as they may require downloading a database and building and compiling separate 3rd-party RNA tools. This becomes challenging for practitioners. Thus, many of these methods provide a web server for use by practitioners. Our model, on the other hand, is end-to-end, only taking MSA as input and outputting the prediction in a single forward pass of the model. Thus, our model can be easily run locally using a simple script, making our work accessible to a wider range of researchers with different technical backgrounds.

Nevertheless, we compare our model to RNAcontact using predictions from its web server. Note that the RNAcontact server will search MSA databases and is likely to use many more MSA sequences compared to our setting, where we use 200 MSA sequences. Moreover, RNAcontact is trained using a much larger dataset with about 300 unique target RNAs, whereas our training set only contains 56 RNAs. However, even with these advantages in favor of RNAcontact, our model still outperforms this SoTA hybrid method (see Table C.1).

D. Comparison with RNA Secondary Prediction Methods

In this study, we investigate RNA contact prediction, a conceptually related but distinct task from secondary structure prediction (Sato et al., 2021; Radford et al., 2021; Szikszai et al., 2022). While secondary structure prediction focuses on identifying nucleotide base pairs connected through hydrogen bonding, contact prediction aims to determine all interactions within a specified distance threshold in the folded RNA structure. As a result, contact prediction can reveal more intricate

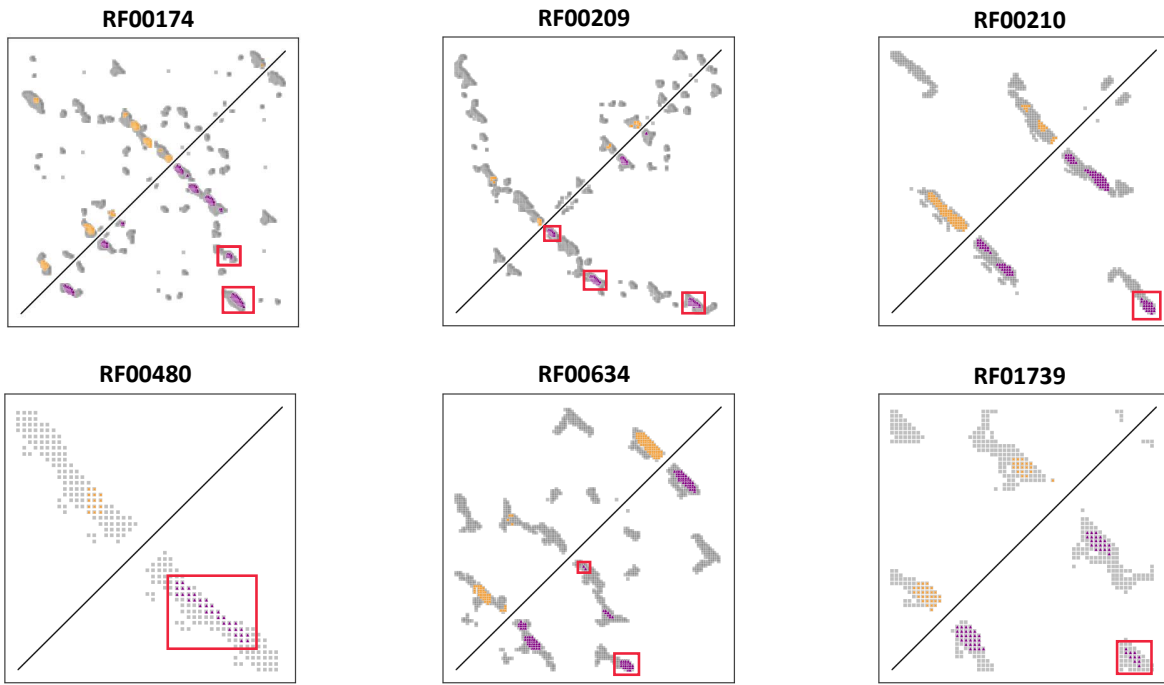


Figure B.1. Visual comparison of contact map predictions by CoCoNet and ours in 6 sample test RNAs. The grey dots denote ground truth contacts, the yellow dots in the upper triangle denote correct predictions by CoCoNet, and the purple dots in the lower triangle denote the correct predictions by ours. The red box highlights correct predictions by our model that are missed by CoCoNet.

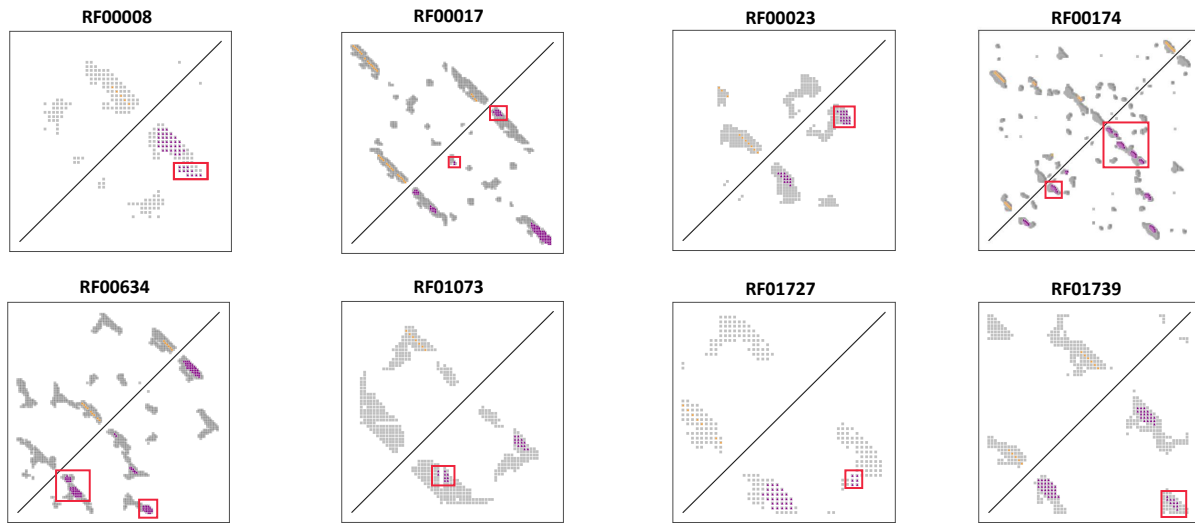


Figure D.1. Visual comparisons between the predictions made by LinearFold and our method. The grey dots represent the ground truth contacts, the yellow dots in the upper triangle represent the correct predictions made by LinearFold, and the purple dots in the lower triangle represent the correct predictions made by our method. The red boxes highlight the correct predictions made by our model that LinearFold missed.

Title Suppressed Due to Excessive Size

Method	PPV _L	PPV _{0.5L}	PPV _{0.3L}
RNAcontact [†]	69.0	81.7	86.7
Ours	73.5	80.6	83.0
Ours (better translation) [‡]	77.3	84.5	88.6

Table C.1. Comparison of our model with RNAcontact, a hybrid approach that uses features extracted by different RNA computational tools in addition to DCA. [†] indicates results obtained using a $\sim 5\times$ larger training set. [‡]: Stronger results by using a different embedding layer for translation nucleotides to amino acids; see additional details in Section 4.2.4.

Method	PPV _L	PPV _{0.5L}	PPV _{0.3L} [†]
LinearFold-C	24.5	49.0	78.1
LinearFold-V	25.9	51.8	79.6
MXfold2	25.7	51.7	83.6
Ours (KDNY translation)	77.3	84.5	88.6

Table D.1. Quantitative comparison of predictions made by LinearFold, MXfold2, and our method. The [†] column shows the PPV for LinearFold and MXfold2, which is calculated as $\frac{1}{|\mathcal{D}|} \sum_{i \in \mathcal{D}} \frac{TP_i}{P_i}$, where TP_i represents true positives and P_i represents the number of predictions. It is worth noting that for LinearFold $P_i \approx 0.30L$ and for MXfold2 $P_i \approx 0.32L$, making it an appropriate comparison to ours when evaluating by PPV_{0.3L}.

details about the RNA tertiary structure.

Specifically, using multiple sequence alignment (MSA) for structural prediction, whether for exclusive pairings in secondary structure or non-exclusive pairings in contact structure, is primarily based on the assumption that structures are more conserved than sequences. This reflects presumably even more fundamental conservation in function. However, the function of a biomolecule is often determined by a cohort of non-exclusive pairings that form the pocket or cavity necessary for its function. Therefore, the predictive power extracted or learned from MSA can extend beyond the simpler exclusive pairings in secondary structure prediction (i.e., the standard base pairs with hydrogen bonds).

Here, we compare our contact prediction approach with two recent secondary structure prediction methods, demonstrating that contact prediction more effectively captures structural characteristics. We observe that secondary prediction methods generate an average of $0.3L$ positive predictions. Thus, a more appropriate comparison utilizes PPV_{0.3L} (using PPV_L would place secondary prediction methods at a disadvantage).

The results shown in Table D.1 (PPV_{0.3L}) indicate that our method outperforms LinearFold and MXfold2. Qualitative analysis and visual comparisons can be found in Figure D.1. By design, secondary structure prediction methods generate a limited number of (secondary) predictions, while our method captures more contacts, many of which come from tertiary contacts.

We note that MXfold2 is a machine learning method. Thus, the appropriate comparison should be performed using the same training set of ours. Nevertheless, we use the MXfold2 server based on the pre-trained model trained using more than 3000 sequences (Sato et al., 2021), and our method shows competitive results.

E. Additional Ablation on Different Nucleotide to Amino Acid Translations

This section presents a more comprehensive set of experiments on various nucleotide to amino acid translations, supplementing the results in Sec.4.2.4. There are approximately 20^4 distinct nucleotide-to-amino acid translations. Although exhaustively examining all combinations is not feasible, we evaluate our method using an alternative set of randomly chosen translations. As demonstrated in Table E.1 A, our method exhibits considerable robustness with respect to the selection of different translations. We also observe that while selecting different amino acids (e.g., DNYK or ACDE) may lead to either strong or weak performance, the permutations of a set of amino acids generally yield similar results. For example, AUCG \rightarrow DNYK, KYND, NYKD, YNDK all perform well. In contrast, AUCG \rightarrow ACDE, CAED, DECA, EDAC all relatively underperform. Based on these experiments, we hypothesize that the transferable contact patterns from the protein transformer CoT to RNA tasks may not rely on an exact translation. It is possible that the richer attention information learned in CoT is preserved for specific sets of amino acids.

Method	PPV _L	PPV _{0.5L}	PPV _{0.3L}
A. Different RNA-to-protein translations			
AUCG → AVIL	66.9	76.3	80.8
AUCG → ILMF	67.0	74.0	78.0
AUCG → RDSC	72.3	81.7	82.7
AUCG → KDSU	73.9	80.4	81.4
AUCG → HETG	75.1	81.2	84.4
AUCG → HDTU	76.2	83.2	86.8
AUCG → KEQG	76.9	80.9	81.4
AUCG → KDTI	76.9	83.6	85.8
AUCG → KDQG	77.3	84.8	87.7
AUCG → KDNU	78.2	86.2	88.0
AUCG → RSKY	78.6	84.3	87.7
AUCG → SDYK	79.8	85.5	87.7
B. Different permutations of KDNY			
AUCG → KYND	74.0	79.8	83.6
AUCG → DNYK	77.0	82.7	85.7
AUCG → NYKD	78.6	83.7	84.5
AUCG → YNDK	80.6	85.2	86.2
C. Different permutations of RDSY			
AUCG → RYSD	77.2	82.3	85.9
AUCG → YRDS	78.9	86.4	90.7
AUCG → DRSY	80.3	85.4	87.1
AUCG → SDYR	81.4	87.2	88.6
D. Different permutations of ACED			
AUCG → EDAC	64.8	70.3	71.7
AUCG → CAED	65.3	72.8	76.0
AUCG → DECA	66.2	76.7	82.7
AUCG → ACDE	68.6	76.9	82.5

Table E.1. Results of different Nucleotide-to-Amino Acid Translations/Mappings for our model. **A.** Despite variations in their performances, the additional translations we explored were competitive compared to the baseline CoCoNet. **B.** We also tested various translations using permutations of KDNY, which showed good results, and **C.** RDSY, which also showed promising outcomes. **D.** However, when we used permutations of ACDE, the results were relatively less competitive.